2026 IEEE/SICE International Symposium on System Integration (SII)
January 11-14, 2026. Cancún, México

Design Concept and Applications of Inflatable Robots: Single and Dual-Arm with Internal Drop-Stitch Structure and Rigid Joints

Gangadhara Naga Sai Gubbala*[1], Hibiki Nakagawa[1], Hiroki Uchida[1], Masato Nagashima[1], Hiroki Mori[2], Young Ah Seong[3], Hiroki Sato[4], Ryuma Niiyama[5], Yuki Suga[6], Tetsuya Ogata[1,7]

***Abstract*— In this research, we focus on the design and applications of a 12DoF(degrees of freedom) dual-arm inflatable robot. The design utilizes a combination of soft bodies, such as inflatable links, and hard joints as servo actuators. This combination enables us to retain the passive safety and compliance of soft robots while leveraging the control accuracy of hard joints. First, we built a 6DoF inflatable arm with a gripper (1DoF). Then, we replicated the single arm to construct a 12DoF dual-arm robot. We then examine the feasibility of this robot for several contact-based tasks, like hammering a nail, pick and place of a handkerchief, and dressing assistance. For our evaluation, we report successful trials and servo faults observed during experiments, as verified by video recordings. With the tasks shown, we confirm the robot's inherent compliance and showcase the qualitative report for the feasibility of contact-rich tasks based on a small number of trials.**

***Index Terms*— Soft Robotics, Dual-Arm Robot, Inflatable Robot, Physical Human-Robot Interaction, Bimanual Manipulation.**

I. INTRODUCTION

For robots that assist and collaborate in our homes to be integrated into daily life, they need to work in close contact with humans and dynamic environmental settings. Therefore, a fundamental design challenge is observed: the trade-off between robot performance and human safety [1], [2], [3].

A wide range of designs can be realized to enhance the safety-performance trade-off. Therefore, the primary components of a robot body (links) and its joints (actuators) will be analyzed. These components can be categorized as hard (high stiffness) or soft (high compliance). One of the combinations is the **Hard Body + Hard Joint** approach, conventionally seen in industrial robots. Although they have high accuracy and efficiency, they are generally kept behind cages as they pose significant collision risks [1]. On the opposite side, we have the **Soft Body + Soft Joint** approach, where the entire body is mostly compliant. Although these systems are safe due to inherent compliance, they need complex control methods because of deformations from their own weight and interaction with surroundings [4], [5].

For understanding the safety, unlike purely active compliance (current/torque/impedance control), which reacts after a contact is detected, our approach uses *passive* body-level compliance. This mitigates impact with zero latency while preserving joint-level controllability [1], [6], [7].

In this paper, we examine the feasibility of our **Soft Body + Hard Joint** robot for contact-rich tasks. First, in Section III, we describe the construction of the single and dual-arm robots. Then, in Section IV, we explain the teleoperation control method. Next, in Section V, we define the experimental tasks and the evaluation metrics, which are the number of successful trials and servo faults observed during experiments and verified from video. In Section VI, we present the results from the experiments, and in Section VII, we discuss the outcomes and limitations. Our main contributions are as follows:

1) The design and construction of a 12DoF inflatable dual-arm robot with soft links and hard joints.
2) A feasibility study showcasing the robot's ability to perform various contact-based tasks by observing task success and servo faults.

II. RELATED WORK

The design and application of soft robots originate from safe contact with humans and surroundings due to their compliant and low-inertia bodies. With an incidental contact, the impact is lowered, but additional complexity is added due to deformation and control difficulty. In the previous studies, flexible joints and soft-rigid combinations with continuous segments are examined [8], [9]. Similarly, we organize our related work with the combination of body and joint type: hard body + hard joint, soft body + soft joint, hard body + soft joint, and soft body + hard joint (this work). Figure 1 shows this map and the region, we explore for everyday contact tasks.

A. Hard Body with Hard Joint

In this combination, we have our commonly used cobots, such as the Universal Robots UR5. To operate safely outside

[1]G. N. S. Gubbala, H. Nakagawa, H. Uchida, M. Nagashima, and T. Ogata are with the Dept. of Intermedia Art and Science, School of Fundamental Science and Eng., Waseda University, Tokyo 169-8555, Japan. Emails: gangadhara@fuji.waseda.jp, hbk.nakagawa@toki.waseda.jp, ogata@waseda.jp.

[2]H. Mori is with the Institute for AI and Robotics, Future Robotics Organization, Waseda University, Tokyo 169-8555, Japan. Email: mori@idr.ias.sci.waseda.ac.jp.

[3]Y. A. Seong is with the Dept. of System Design, Faculty of Eng. and Design, Hosei University, Tokyo 102-8160, Japan. Email: seong@hosei.ac.jp.

[4]H. Sato is with the School of Project Design, Miyagi University, Miyagi 981-3300, Japan. Email: satoh@myu.ac.jp.

[5]R. Niiyama is with the School of Science and Technology, Meiji University, Kanagawa 214-8571, Japan. Email: niiyama@meiji.ac.jp.

[6]Y. Suga is with Waseda Research Institute for Science and Engineering (WISE), Waseda University, Tokyo 169-8555, Japan, and also with Sugar Sweet Robotics (SSR). Email: ysuga@ysuga.net.

[7]T. Ogata is also with the National Institute of Advanced Industrial Science and Technology (AIST), Tokyo 100-8921, Japan. Also, Director of the Institute for AI and Robotics at Waseda University. Also a Visiting Professor at the National Institute of Informatics (NII).

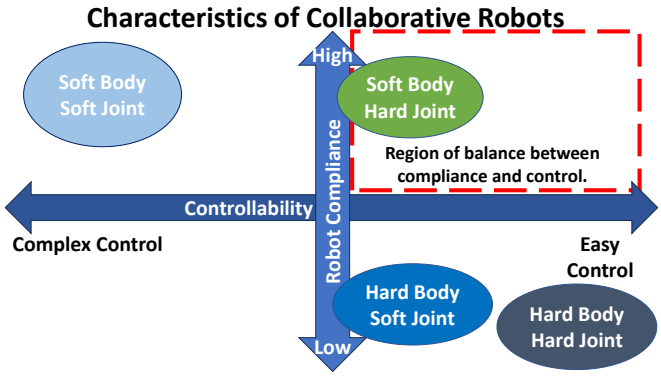

Fig. 1: In this plot, we show a high-level understanding of robot designs with trade-offs between compliance and controllability. We propose that our soft body + hard joint approach occupies region which balances passive collision safety with joint-level control for everyday contact tasks.

of cages, especially near humans, these robots must strictly manage collision forces. Global safety standards like ISO 10218-1 and application-specific guidelines for power-and-force limiting (PFL) such as ISO/TS 15066 decide the design and operation of cobots [10], [11]. Recent studies show that achieving both precision and safety requires limiting speed and actuator capacity, especially during incidental contact [6], [12]. This limiting of speed and actuator capacity is identified from several biomechanical studies that are determined by the upper threshold of an impact, acceptable from a robot when it comes into contact with humans [13], [14].

B. Soft Body with Soft Joint

Inherent safety is observed in soft robots due to their low inertia and compliance, making them naturally safe for contact. Although recent trends show good advances in Soft Robotics, the difficulties due to deformations are still present to establish proper control and efficient speed to accomplish everyday tasks [15], [16]. Physical Human-Robot interaction is best suitable for inflatable and other soft body structures because of almost zero latency for incidental contacts, and low inertia mitigates these forces. However, controllability remains a challenge because of deformations due to external forces, due to their inability to maintain their shape [15], [17].

C. Hard Body with Soft Joint

One of the methods used is with series elastic actuators (SEAs) to utilize a spring for compliance at the driveline. Although this improves impact tolerance, it can reduce positional accuracy and precision if not carefully controlled [7], [18]. Another alternative method using spring compliance is the Series Clutch Actuator (SCA), which instead uses a controllable clutch. This gives passive safety along with adjustable torque limits, and full back-drivability when we disengage the clutch [19]. In another research, just adding purely passive padding versus active sensing skin alone reduces impact forces by 40% even before the control reacts at the moment of contact [20].

D. Soft Body with Hard Joint (This Work)

In our approach, we assign safety and controllability to each of the components separately. The soft body provides passive safety because of their deformations, and the rigid servo joint provides joint-level actuation. This design helps us stay within the contact-based pHRI limits of biomechanical pain tolerance when incidental contact may occur [21]. On the other hand, completely soft robots cannot maintain their shape under external force and are difficult to use for day-to-day tasks.

E. Inflatable Soft Robots

In the previous research, we can see Sanan et al. [22] constructed a 2link inflatable polyurethane arm, that inspired a fictional safe inflatable health care robot “Baymax”, [23]. Lightweight helium-filled, multi-DoF inflatable robot arm was used for surveillance in disaster-prone areas was introduced by Takeichi et al. [24]. Alspach et al. showcased air-filled sensors for a soft hand arm system designed for human-robot interaction.[25]. Gillespie et al. [26] constructed “King Louie”, a fabric-based inflatable humanoid robot funded by NASA for future space missions because of its lightweight and compact design. Niiyama et al.’s [27] explored joint mechanisms for a continuous blow-powered robot. Although the previous show potential for contact-based tasks. They cannot maintain their shape under external forces during contact [15], [17].

Hence we introduce inflatable structures that use internal Drop stitch structure that distribute loads and better preserve shape under external force (POIMO) [28]. Because of the external force, the volume reduces and pressure increases keeping ($pV = \text{const}$), and the tension in the threads helps to distribute the force across the surface of the balloon [29]. To further analyze, we previously conducted dynamic motion capture analysis for 1DoF and 2DoF balloons undergoing sinusoidal motion. The results show complex, nonlinear deformations and make the prediction of end-effector position challenging [30]. In comparison with rigid cobots that entirely rely on active sensing and control, our combination provides passive, initial contact safety with low latency reaction time. We show the feasibility for real-life tasks and the ability to maintain contact on hard surfaces in this paper from our demonstrations.

III. ROBOT CONSTRUCTION

The inflatable robot is constructed from commercially available Dynamixel servo motors from ROBOTIS [31] and a custom-designed balloon with drop-stitch structure. The current design is built on top of our previous work of a 3DoF 2link inflatable robot with a combination of soft links and rigid joints [29]. Every link is made from two base cloth fabrics with a thermoplastic polyurethane (TPU) coating. The top and bottom cloth fabrics are connected with polyester threads or yarn, which help in preventing bending as shown in Fig. 2a. The next step was the connection between the soft body and the rigid joint, made by a ”balloon plate” that is fixed onto a balloon surface with adhesive, and

another ”mediator plate” is used to interconnect the balloon plate to the servo frame, as shown in Fig. 2c. To realize

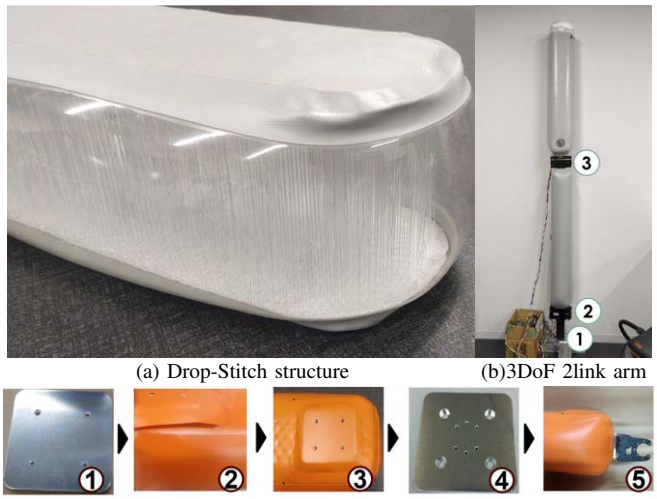

(a) Drop-Stitch structure (b)3DoF 2link arm

(c) Actuator attachment process: Soft body + hard joint

Fig. 2: (a) To visualize the Drop-Stitch structure of the Transparent balloon sample. (b) The design result of base (1), shoulder (2), and elbow (3) servo joints from the result of 3DoF 2link inflatable robot payload test [29] (c) Interconnection process for soft body to rigid joint. (1) With an adhesive, the balloon plate (1) is fixed to a fabric piece (2), then attached to the balloon (3). Another metal plate called “mediator plate” (4) connects the soft body (inflatable link) with the rigid joint (servo frame) (5) [29].

the 3DoF arm structure, we have conducted payload tests on a single link balloon with weights placed at different orientations and ”top-bottom” placement on the cuboidal links. This orientation has better resilience to recover back to the original shape as shown in Fig. 3 [29]. The single-

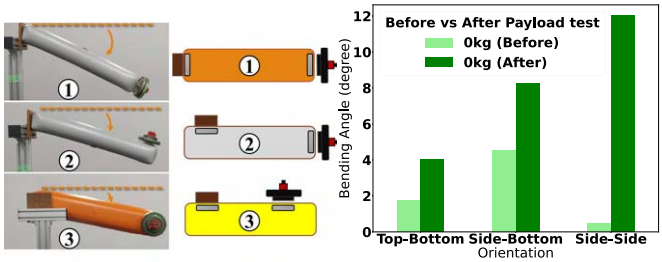

(a) Payload test(PT) (b) Before and After Evaluation

Fig. 3: (a) This shows three loading orientations based on the fixed end of the balloon to the payload part of the balloon. We apply a payload to see how well the balloon returns to its original shape in each position. The balloon orientations are (1) top-bottom, (2) side-bottom, and (3) side-side. (b) This graph compares the balloon’s bending angle before and after the payload test for different orientations. The y-axis shows the bending angle in degrees. The top-bottom orientation shows the least deformation, indicating the best resilience. This plot is taken from our previous research [29].

arm is built by adding a wrist and gripper to the 3DoF arm. This makes the arm a 6DoF arm + gripper (1DoF), which consists of two drop-stitch balloon links connected by rigid servo motors. The visualized arm schema is shown in Fig. 4.

To realize the maximum payload, we calculated the torque for each joint, shown in Table I for the worst case scenario. The calculations of worst case orientation have given a 1.4 kg payload. The shoulder joint would experience the highest torque, followed by the elbow joint. Hence, we opted for a high torque servo (ROBOTIS PH54-200-S500-R) with a 44.7 Nm stall torque. The remaining five joints utilized XM540-W150-R servos with a 7.3 Nm stall torque.

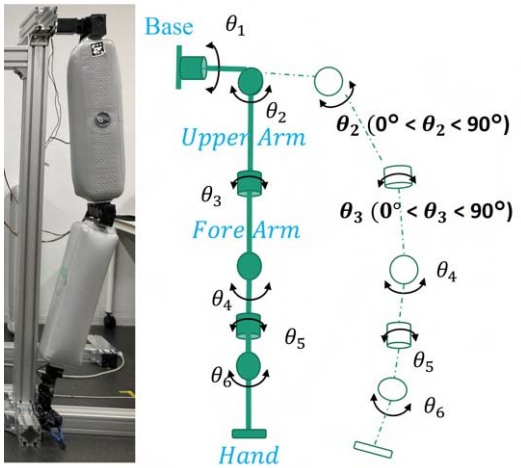

Fig. 4: The robot schema for a 6DoF single-arm inflatable robot is shown with an upper arm, forearm, and wrist. The left image is of the actual robot, and the right is the kinematic structure with the angle ranges of the inflatable arm.

To perform more complex tasks in day to day life, we extended our design to a 12DoF dual-arm robot (Fig. 5). The construction is done by mirroring and replicating the single-arm structure. This dual-arm configuration helps with complex coordination, such as holding an object with one hand while the other performs some task [32].

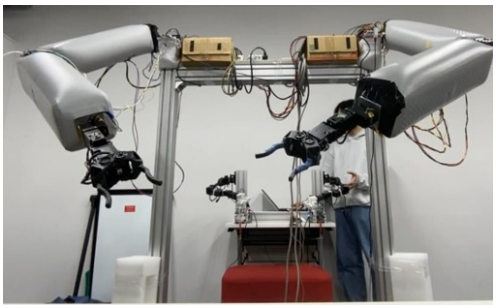

Fig. 5: For the 12DoF inflatable dual-arms, we mirrored and replicated single-arm structure. The distance between the two arm bases is set to 90 cm to create enough workspace and reduce frequent accidental contact.

IV. CONTROL METHOD

In the previous research, we have mainly used only sinusoidal motion, and relying only on waypoints is not suitable for complex tasks [30]. Hence, we moved to a unilateral leader-follower teleoperation system. This approach allows for a more intuitive human control. But it is challenging to synchronize the operator’s movements on a low-torque leader device with the high-torque and higher resolution follower servos. The operator’s movements have natural jitter or shaking, leading to a high-frequency, noisy signal. To overcome this, we applied a second-order low-pass filter with a 2.0 Hz cutoff frequency to the converted angle commands from the leader for a smooth motion of the follower. The leader-follower system uses only position control in angle space.

TABLE I: Calculated torque of each servo motor for a 1.4 kg payload at the arm tip (worst-case posture).

Joint	Servo Model	Stall Torque (N m)	% of Max	Axial Load (N)	% of Max	Radial Load (N)	% of Max
1 (Base yaw)	PH54-200	–	–	52.0	40.0%	–	–
2 (Shoulder pitch)	PH54-200	43.6	97.5%	–	–	43.6	11.8%
3 (Shoulder roll)	PH54-200	15.6	34.9%	–	–	26.9	7.3%
4 (Elbow pitch)	XM540	1.56	14.7%	17.0	84.8%	–	–
5 (Wrist pitch)	XM540	0.85	8.0%	–	–	15.3	38.3%
6 (Wrist roll)	XM540	0.69	6.5%	–	–	13.7	34.3%

The leader device has the same structure as the follower for the single-arm system, as shown in Fig. 6. For the dual-arm leader system, we similarly replicated the follower structure to control both arms simultaneously (Fig. 7). To improve the usability of dual-arm operation, the leader is held by elastic bands attached above the frame so the leader does not fall under its own weight, and no torque control is used on the leader (Fig. 8b). For easy gripper control, we have finger mounts (Fig. 8a), that allow for more comfortable and sustained teleoperation.

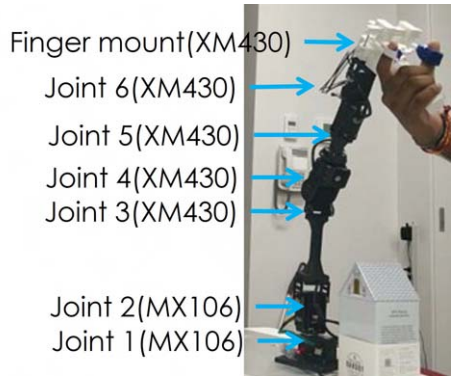

Fig. 6: The components and the structure of the single-arm leader device, with details of all the joints and the specific servo motors utilized. This rigid leader controller has a finger mount as the end-effector, allowing intuitive control.

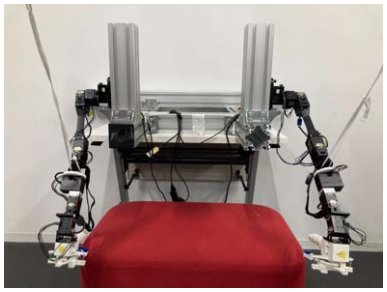

Fig. 7: The components and the structure of the dual-arm leader device, which is made by mirroring and replicating the single-arm design. This rigid leader controller has a finger mount gripper as the end- effector, allowing the operator to intuitively control both the arm's pose and its grasping action

V. EXPERIMENTAL METHOD

A. Scope and Evaluation

In this work, we primarily focus on the high-level tasks to obtain a qualitative analysis on a small number of trials. Evaluation criteria are as follows:

- **Successful Trial** is achieved only if the primary objective as described in the task criteria is fulfilled.
- **Servo Fault** servo motor's protection mode is initiated due to exceeding its operational limits, causing the program and motion to completely stop. If an error is identified, the whole robot is kept in stop mode.

(a) (b)

Fig. 8: The dual-arm leader device components, showing (a) Aloha-inspired 3D-printed components for hand control [33] and (b) the elastic cords used for the gravity compensation to ease the operation of leader follower system.

The evaluation is done by direct observation and rechecking of frame by frame review of the recorded videos. A servo fault was confirmed by the sudden stop of the entire robot's motion, in direct observation and video. For each task, we counted successful trials and servo faults for the total trials conducted.

B. Task Criteria

The success criteria for each task are given as follows:

- **Handkerchief Pick-and-Place** is confirmed successful if fully lifted from the table and successfully placed into the target basket.
- **Nailing** is confirmed successful if the hammer head successfully hits the nail head.
- **Payload Stability test** is performed if the arm holds the specified weight for at least 3 seconds without a rocking motion.
- **Towel Folding** is confirmed successful if the two edges of the towel are brought together with a final misalignment of less than 3 cm.
- **Scarf Wrapping** is confirmed successful if the scarf completes one full loop around the mannequin's neck, and the ends are almost equal in length.
- **Coat Dressing** is confirmed successful if the coat is successfully placed on the mannequin's shoulders and does not fall off.
- **Chair Lifting** is confirmed successful if the chair is lifted such that it's off the floor and held for a minimum of 3 seconds.

VI. EXPERIMENTAL RESULTS

To confirm the properties of the contact tolerance of our design, we conducted a series of demonstrations. In the

following subsections, we describe the qualitative per-trial results with remarks where applicable.

A. Single-Arm Task Results

The 6DoF single-arm was used to check the feasibility of simple tasks like Handkerchief Pick-and-Place, Nailing, and Payload Stability test. Each trial outcomes are shown in Table II and Table III.

1) Handkerchief Pick-and-Place: This task is inspired by the challenges faced by a rigid robot to perform tasks like picking and placing a handkerchief from a hard surface. The rigid robot either needs to have a compliant mechanism or the actuators will reach failure with constant contact with the hard surface[34]. We hypothesize that our design can withstand contact with a hard surface and manipulate a delicate object. The robot task was to pick up a handkerchief from the top of a table, as shown in Fig. 9. We teleoperated to pick the handkerchief, and the operator to hold the hankey, the target was "overshoot", allowing the gripper to press directly against the table without damage. In total, the robot performed well in 2 of 3 trials, with 0 servo faults observed.

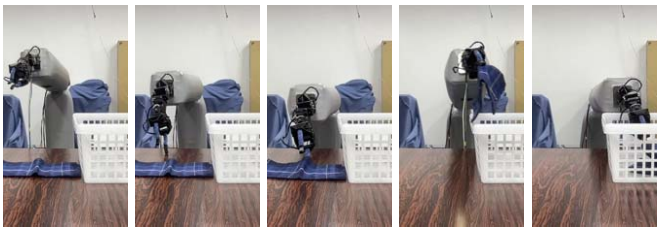

t=0s t=4s t=8s t=12s t=16s

Fig. 9: The Handkerchief Pick-and-Place task performed with teleoperation. At t=8s, the robot gripper makes constant contact with the table to position itself correctly for picking the handkerchief. Although the operator exerts excess force, the robot's soft balloon body absorbs the additional force without disabling the servo motors, allowing it to complete the task and successfully place the handkerchief in the basket.

2) Nailing or hammering: To check the robustness of the design, we performed repeated impact nailing tasks. A wooden mallet was attached to the robot's end-effector, and it is teleoperated so the arm can strike a nail's head, as shown in Fig. 10. At time of impact, the inflatable structure compressed which is observed visually, and reduced the shock forces. We observed 16 successes in 20 strikes, with 1 servo fault that occurred at the moment of impact and 3 missed to strike the head.

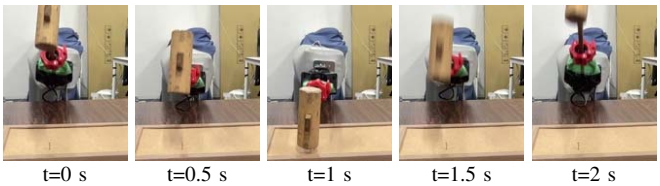

t=0 s t=0.5 s t=1 s t=1.5 s t=2 s

Fig. 10: A small nail is first fixed on a wooden board, and we teleoperated the arm to strike it on the nail head. At every impact, the inflatable structure compresses and continues to strike the nail. One of the successful trials is shown out of the 20 trials.

3) Payload test for single-arm: For a baseline of payload capacity, the single-arm robot lifted increasing weights (Fig. 11). The robot is set to lift 0.5, 1, and 1.5 kg. When lifted with 0.5 kg, it was stable for 1 kg, there was minor rocking, but with the 1.5 kg weight, the balloon link deformed significantly, leading to failure. The robot was successful in 2 of 2 trials with 0.5 kg, 1 of 2 trials with 1.0 kg, and 0 of 2 trials with 1.5 kg. No servo faults were observed.

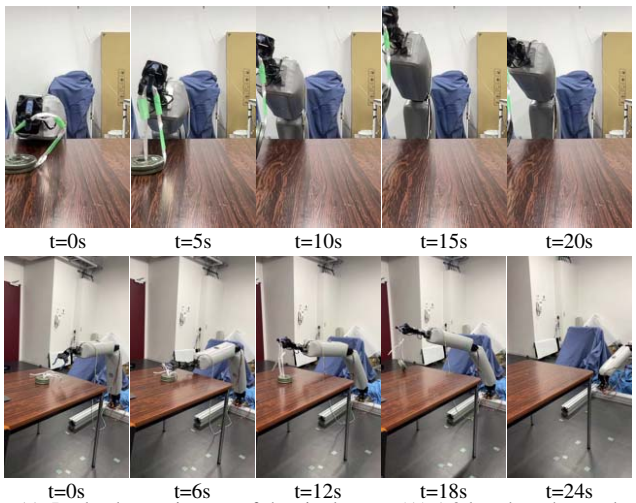

A

t=0s t=5s t=10s t=15s t=20s

B

t=0s t=6s t=12s t=18s t=24s

Fig. 11: Payload capacity test of the single-arm. (A) 1.0 kg: the robot rocks initially, then reaches steady state. (B) 1.5 kg: by t=18s the center of mass shifts, then the arm bends in the opposite direction by t=24s.

TABLE II: Per-trial outcomes for Single-Arm Manipulation.

Task	Trial	Success(1/0)	Fault(1/0)	Remarks
Handkerchief	1	1	0	–
	2	1	0	–
	3	0	0	Dropped at transfer
Nailing	1-20	16	1	Fault on strike #13

TABLE III: Per-trial outcomes for Single-Arm Payload test.

Weight	Trial	Success(1/0)	Fault(1/0)	Remarks
0.5 kg	1	1	0	Stable hold
0.5 kg	2	1	0	Stable hold
1.0 kg	1	1	0	Minor rocking
1.0 kg	2	0	0	Unstable rocking
1.5 kg	1	0	0	Dropped
1.5 kg	2	0	0	Dropped

B. Dual-Arm Task Results

We perform more complex day to day tasks like Towel folding, Dressing Assistance, and Chair Lifting with a 12DoF dual-arm robot. In the following subsections, we describe the qualitative per-trial results with remarks where applicable, as shown in Table IV.

1) Towel Folding: We showcase the dual-arm robot's coordinated manipulation with the towel folding task (Fig. 12). The robot's inflatable arms frequently come into contact with each other and the table. These contact events did not interrupt the task. The robot succeeded in 2 of 3 trials, with

Fig. 12: The towel folding task is teleoperated to fold the towel in half, tolerating constant contact with the table. The task used only position control based on the feedback from the human operator's vision, with no force feedback. Incidental contact happened with the table and between the arms, which did not result in any servo faults.

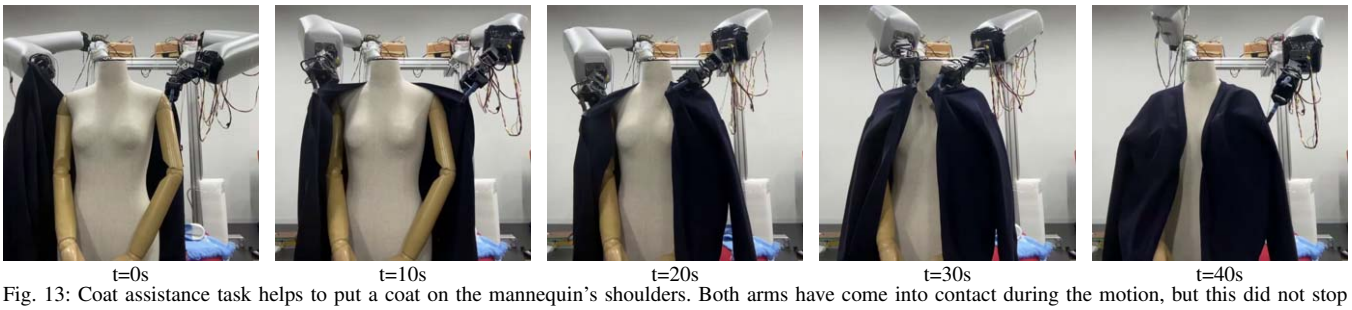

Fig. 13: Coat assistance task helps to put a coat on the mannequin's shoulders. Both arms have come into contact during the motion, but this did not stop the teleoperation, as the impact was absorbed by the robot's compliant body.

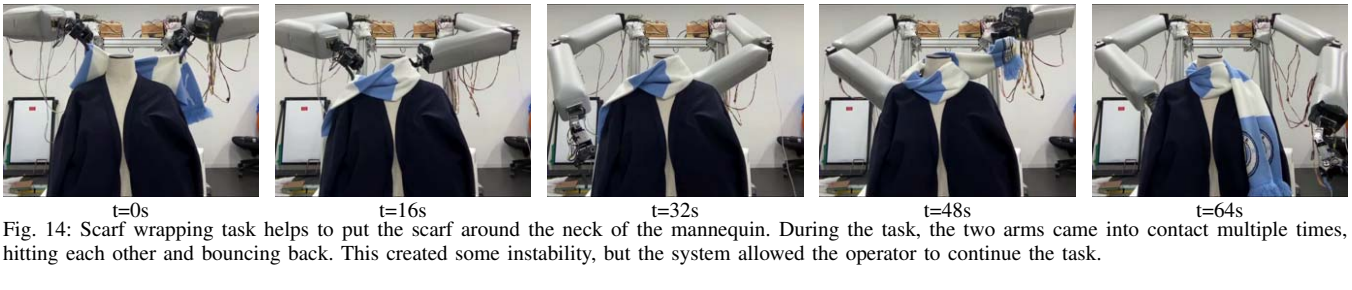

Fig. 14: Scarf wrapping task helps to put the scarf around the neck of the mannequin. During the task, the two arms came into contact multiple times, hitting each other and bouncing back. This created some instability, but the system allowed the operator to continue the task.

0 servo faults. The failure was due to the slipping of the towel.

2) Dressing Assistance: To showcase safe operation for assisting humans, especially the elderly, we performed dressing assistance on a mannequin. The dressing assistance has two parts, placing a coat (Fig. 13) and wrapping a scarf (Fig. 14). The coat dressing was successful in 2 of 2 trials, and the scarf wrapping succeeded in 1 of 2 trials. The failure was due to the slipping of the scarf. No servo faults were detected.

3) Chair Lifting: The dual-arms have balloons of slightly different shapes due to the manufacturing and the repeated use of the balloons, which changes the shape at different places. Hence, symmetry cannot be guaranteed. To check if the dual-arm can sustain lifting a heavy object without triggering servo failure. We perform this task to evaluate cooperative lifting of a 4.3 kg object, a mass that exceeds the reliable 1.0 kg capacity of a single-arm. We demonstrated this by lifting the chair, as shown in Fig. 15. The dual-arm system successfully lifted the chair by coordinating both arms. The task succeeded in 2 of 2 trials, with no servo faults.

An overall summary of all the results of experimental tasks is provided in Table V.

TABLE IV: Per-trial outcomes for Dual-Arm Tasks.

Task	Trial	Success(1/0)	Fault(1/0)	Remarks
Towel Folding	1	1	0	–
	2	1	0	–
	3	0	0	Missed
Scarf Wrapping	1	1	0	–
	2	0	0	Scarf slipped
Coat Dressing	1	1	0	–
	2	1	0	–
Chair Lifting	1	1	0	Stable lift
	2	1	0	Stable lift

TABLE V: Summary of Experimental Feasibility Results.

Task	Arm	Trials (N)	Successes	Faults
Handkerchief	Single	3	2	0
Nailing	Single	20	16	1
Payload (0.5 kg)	Single	2	2	0
Payload (1.0 kg)	Single	2	1	0
Payload (1.5 kg)	Single	2	0	0
Towel Folding	Dual	3	2	0
Scarf Wrapping	Dual	2	1	0
Coat Dressing	Dual	2	2	0
Chair Lifting	Dual	2	2	0

VII. DISCUSSION

Overall, the experiments qualitatively indicate that the inflatable robot is a feasible approach for high contact

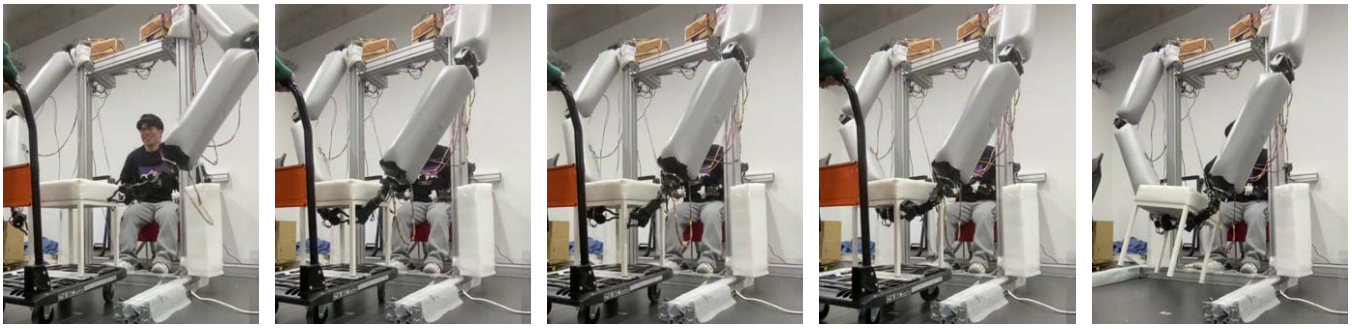

Fig. 15: Operator lifts a heavy object, and due to the inherent asymmetry in the balloon manufacturing process, the link deformations were not identical. We tested this to see how the system would manage the load and whether faults would occur, but no servo faults were detected during the cooperative lift.

tolerance. The results show our approach can complete a variety of tasks with few servo faults, validating our soft-body and hard-joint design. The robot's passive compliance from inflatable links tolerates incidental contact, and the servo joint actuation helps task-level controllability.

First, the inherent compliance was clearly applicable in the handkerchief and dressing assistance tasks. The robot's material compliance lets it tolerate unplanned contact without damage or danger. This focuses the safety burden from complex software control to a predictable hardware capability.

Second, the towel folding task showed the importance of constant contact and ease for the operator to achieve the task objective. The ability of the robot to tolerate both self-contact and environmental contact without failure is a major advantage over hard robot systems. This helps for robust operation in cluttered, real-world environments like our homes and human surroundings.

Third, the chair lifting task provided a clear advantage through bimanual cooperation, showing that the dual-arm configuration can help with tasks that may cause asymmetry.

This study clearly has several limitations. First, the number of trials for each task is small, so the results indicate possibility rather than providing a statistical measure of performance. Second, the outcome labeling is based on direct observation, with video recordings serving as the verifiable record, which lacks the precision of automated sensor data. Finally, without contact sensors, we can only qualitatively note the timing of faults relative to contact events.

VIII. CONCLUSION AND FUTURE WORK

In this research, we showed that the combination of soft body with a rigid joint can demonstrate effective results with high contact tolerance. The development of 6DoF single-arm and 12DoF dual-arm, servo-actuated inflatable robots has shown complex tasks involving deformable objects, repeated impacts, and constant contact in a qualitative feasibility setting. To further analyze it, we would require a direct comparison with a rigid arm of similar dimensions for the future work.

In future work, we will directly address the limitations of this study. Next, we aim to collect a large number of trials for each task to enable more robust quantitative analysis. We plan to integrate contact sensors into the robot's links to precisely measure interaction force feedback and calculate the rate of faults during contact. We also plan to conduct a comparative study against a rigid robot to evaluate the benefits of our compliant design. Finally, we will perform the demonstrated tasks with the help of machine learning to expand on our previous research on wiping with LSTM models [29].

ACKNOWLEDGMENT

JST Moonshot R&D Program JPMJMS2031 supported this work. The authors would like to thank all collaborators and contributors to this project.

REFERENCES

[1] S. Haddadin, A. Albu-Schäffer, and G. Hirzinger, "Safe physical human-robot interaction: Measurements, analysis and new insights," in *Robotics Research*, M. Kaneko and Y. Nakamura, Eds., Berlin, Heidelberg: Springer Berlin Heidelberg, 2011, pp. 395–407, ISBN: 978-3-642-14743-2.

[2] S. Li, N. Figueroa, A. J. Shah, and J. A. Shah, "Provably safe and efficient motion planning with uncertain human dynamics," in *Robotics: Science and Systems XVII*, 2021.

[3] S. Haddadin and E. Croft, "Physical human-robot interaction," in *Springer Handbook of Robotics*, B. Siciliano and O. Khatib, Eds. Cham: Springer International Publishing, 2016, pp. 1835–1874. DOI: 10.1007/978-3-319-32552-1_69.

[4] C. M. Best, J. P. Wilson, and M. D. Killpack, "Control of a pneumatically actuated, fully inflatable, fabric-based, humanoid robot," in *Proc. IEEE-RAS Int. Conf. Humanoid Robots (Humanoids)*, 2015, pp. 1133–1140.

[5] M. Takeichi, K. Suzumori, G. Endo, and H. Nabae, "Development of giacometti arm with balloon body," *IEEE Robot. Autom. Lett.*, vol. 2, no. 2, pp. 951–957, 2017.

[6] A. Zacharaki, I. Kostavelis, A. Gasteratos, and I. Dokas, "Safety bounds in human robot interaction: A survey," *Safety science*, vol. 127, p. 104 667, 2020.

[7] J. L. de Gea Fernández, B. Yu, V. Bargsten, M. Zipper, and H. Sprengel, "Design, modelling and control of novel series-elastic actuators for industrial robots," *Actuators*, vol. 9, no. 1, p. 6, 2020.

[8] B. Yu, "Design, modeling, and control of robots with link or joint flexibilities," Ph.D. dissertation, Universität Bremen, 2025.

[9] B. Yu and S. Natarajan, "An easy use auxiliary arm: Design and control of a portable continuum manipulator for enhanced dexterity by soft-rigid arms collaboration," in *2020 3rd IEEE International Conference on Soft Robotics (RoboSoft)*, 2020, pp. 164–169.

[10] *Iso 10218-1:2025 robotics - safety requirements - part 1: Industrial robots*, International Organization for Standardization, 2025. [Online]. Available: https://www.iso.org/standard/73933.html.

[11] *Iso/ts 15066:2016 robots and robotic devices - collaborative robots*, International Organization for Standardization, 2016. [Online]. Available: https://www.iso.org/standard/62996.html.

[12] W. Li, Y. Hu, Y. Zhou, and D. T. Pham, "Safe human–robot collaboration for industrial settings: A survey," *J. Intell. Manuf.*, vol. 35, no. 2, pp. 893–919, 2024.

[13] R. Behrens, G. Pliske, M. Umbreit, S. Piatek, F. Walcher, and N. Elkmann, "A statistical model to determine biomechanical limits for physically safe interactions with collaborative robots," *Front. Robot. AI*, vol. 8, p. 667 818, 2022.

[14] D. Han, M. Y. Park, J. Choi, H. Shin, R. Behrens, and S. Rhim, "Evaluation of force pain thresholds to ensure collision safety in worker–robot collaborative operations," *Front. Robot. AI*, vol. 11, p. 1 374 999, 2024.

[15] O. Yasa et al., "An overview of soft robotics," *Annual Review of Control, Robotics, and Autonomous Systems*, vol. 6, no. 1, pp. 1–29, 2023.

[16] Y. Wang, Y. Wang, R. T. Mushtaq, and Q. Wei, "Advancements in soft robotics: A comprehensive review on actuation methods, materials, and applications," *Polymers*, vol. 16, no. 8, p. 1087, 2024.

[17] D. Rus and M. T. Tolley, "Design, fabrication, and control of soft robots," *Nature*, vol. 521, no. 7553, pp. 467–475, 2015.

[18] F. Sanfilippo, M. Økter, J. Dale, H. M. Tuan, M. H. Zafar, and M. Ottestad, "Open-source design of low-cost sensorised elastic actuators for collaborative prosthetics and orthotics," *HardwareX*, vol. 19, e00564, 2024.

[19] S. Kulkarni, A. Schmitz, S. Funabashi, and S. Sugano, "Development and evaluation of a linear series clutch actuator for vertical joint application with static balancing," in *2020 IEEE/RSJ International Conference on Intelligent Robots and Systems (IROS)*, 2020, pp. 6353–6360. DOI: 10.1109/IROS45743.2020.9341293.

[20] P. Svarny et al., "Effect of active and passive protective soft skins on collision forces in human–robot collaboration," *Rob. and Comp-Int. Manuf.*, vol. 78, p. 102 363, 2022, ISSN: 0736-5845.

[21] M. Farajtabar and M. Charbonneau, "The path towards contact-based physical human–robot interaction," *Robot. Auton. Syst.*, vol. 171, p. 104 829, 2024.

[22] S. Sanan, P. S. Lynn, and S. T. Griffith, "Pneumatic torsional actuators for inflatable robots," *J. Mech. Robot.*, vol. 6, 2014.

[23] D. Hall, C. Williams, J. Roberts, R. L. Baird, and D. Gerson, *Movie: Big hero 6*, Directed by D. Hall & C. Williams; produced at Walt Disney Animation Studios, Burbank, CA, 2015.

[24] M. Takeichi, K. Suzumori, G. Endo, and H. Nabae, "Development of a 20-m-long giacometti arm with balloon body based on kinematic model with air resistance," in *Proc. IEEE/RSJ Int. Conf. Intell. Robots Syst. (IROS)*, 2017, pp. 2710–2716.

[25] A. Alspach, J. Kim, and K. Yamane, "Design and fabrication of a soft robotic hand and arm system," *IEEE Int. Conf. Soft Robot. (RoboSoft)*, pp. 379–385, 2018.

[26] M. T. Gillespie, C. M. Best, and M. D. Killpack, "Simultaneous position and stiffness control for an inflatable soft robot," in *Proc. IEEE Int. Conf. Robot. Autom. (ICRA)*, 2016, pp. 1095–1101.

[27] R. Niiyama, Y. Seong, Y. Kawahara, and Y. Kuniyoshi, "Blower-powered soft inflatable joints for physical human-robot interaction," *Front. Robot. AI*, vol. 8, 2021.

[28] H. Sato et al., "Soft yet strong inflatable structures for a foldable and portable mobility," in *Ext. Abstr. CHI Conf. Hum. Factors Comput. Syst.*, 2020, pp. 1–4.

[29] G. N. S. Gubbala et al., "Augmenting compliance with motion generation through imitation learning using drop-stitch reinforced inflatable robot arm with rigid joints," *IEEE Robot. Autom. Lett.*, vol. 9, no. 10, pp. 8595–8602, 2024.

[30] G. N. S. Gubbala et al., "Deformation analysis and prediction of drop-stitch reinforced inflatable robot link for 1dof and 2dof motion," in *2025 IEEE/SICE International Symposium on System Integration (SII)*, 2025, pp. 88–95.

[31] ROBOTIS, *Robotis e-shop*, https://e-shop.robotis.co.jp/.

[32] C. Smith et al., "Dual arm manipulation - a survey," *Robotics and Autonomous systems*, vol. 60, no. 10, pp. 1340–1353, 2012.

[33] T. Z. Zhao, V. Kumar, S. Levine, and C. Finn, "Learning fine-grained bimanual manipulation with low-cost hardware," in *Robotics: Science and Systems XIX*, 2023.

[34] P. Yang, K. Sasaki, K. Suzuki, K. Kase, S. Sugano, and T. Ogata, "Repeatable folding task by humanoid robot worker using deep learning," *IEEE Robot. Autom. Lett.*, vol. 2, no. 2, pp. 397–403, 2017.